

# Thermal Properties of Carbon Nanotube–Copper Composites for Thermal Management Applications

Ke Chu · Hong Guo · Chengchang Jia ·  
Fazhang Yin · Ximin Zhang · Xuebing Liang ·  
Hui Chen

Received: 20 October 2009 / Accepted: 5 March 2010 / Published online: 19 March 2010  
© The Author(s) 2010. This article is published with open access at Springerlink.com

**Abstract** Carbon nanotube–copper (CNT/Cu) composites have been successfully synthesized by means of a novel particles-compositing process followed by spark plasma sintering (SPS) technique. The thermal conductivity of the composites was measured by a laser flash technique and theoretical analyzed using an effective medium approach. The experimental results showed that the thermal conductivity unusually decreased after the incorporation of CNTs. Theoretical analyses revealed that the interfacial thermal resistance between the CNTs and the Cu matrix plays a crucial role in determining the thermal conductivity of bulk composites, and only small interfacial thermal resistance can induce a significant degradation in thermal conductivity for CNT/Cu composites. The influence of sintering condition on the thermal conductivity depended on the combined effects of multiple factors, i.e. porosity, CNTs distribution and CNT kinks or twists. The composites sintered at 600°C for 5 min under 50 MPa showed the maximum thermal conductivity. CNT/Cu composites are considered to be a promising material for thermal management applications.

**Keywords** Metal–matrix composites · Carbon nanotubes · Spark plasma sintering · Thermal conductivity

## Introduction

Carbon nanotubes (CNTs) possess a unique structure and properties that have attracted significant interest worldwide [1, 2]. Research in potential CNTs application fields including energy storage, molecular electronics, nanopores, sensor and composite materials has developed very quickly and shows a promising future [3].

When single-wall carbon nanotubes (SWCNTs) or multi-wall carbon nanotubes (MWCNTs) are incorporated in numerous composite systems, including the metal, polymer and ceramic as matrices, newly excellent mechanical, electrical and thermal properties of the composites can be obtained. Over the past decade, a larger portion of researches have been focused on the development of CNT-reinforced polymer [4–6] and ceramic [7–9]-based composites. The incorporation of CNTs into metal–matrix has become a new focus in recent years [10–13]. One main application of CNTs is as a reinforcing agent to improve the mechanical properties of the metal–matrix composites (MMCs) by taking advantage of their outstanding mechanical properties such as elastic modulus ( $\sim 1$  TPa) and tensile strength ( $\sim 150$  GPa), which is a research hot spot at present. Cha et al. [10] reported a 200% increase in the yield strength in 10 vol.% CNT-reinforced Cu composites. Noguchi et al. [11] found a sevenfold increase in compressive yield strength in 1.6 vol.% CNT/Al composites. Laha et al. [12] obtained a 71.8% increase in microhardness in CNT/6061Al composites when 10 wt. % CNTs was added. Carreno-Morelli et al. [13] showed that the Young's modulus was increased by 9% in CNT/Mg composites with addition of 2 wt. % CNTs. As for these CNT/metal composites, the orientation of the CNTs, homogeneity of the composite, nanotube aspect ratio and the volume fraction of nanotubes are expected to have significant influences on the properties

K. Chu (✉) · H. Guo · F. Yin · X. Zhang  
National Engineering and Technology Research Center  
for Non-Ferrous Metals Composites, General Research Institute  
for Nonferrous Metals, 100088 Beijing, China  
e-mail: siny@yahoo.com.cn

C. Jia · X. Liang · H. Chen  
School of Material Science and Engineering, University  
of Science and Technology Beijing, 100083 Beijing, China

of the nanocomposite [14, 15]. Controlling such factors to obtain an exceptional composite is very challenging. Furthermore, given the excellent thermal properties of CNTs like extraordinarily low coefficient of thermal expansion ( $\approx 0.10^{-6}/\text{K}$ ) [16] and ultra-high thermal conductivity (3,000–6,000 W/mK) [17] in combination with the superior electrical and thermal conductivities of the copper, CNTs-reinforced Cu matrix (CNT/Cu) composites are very attractive to meet the increasing demands for high performance thermal management materials used in heat sinks and electronic packages. However, most effects have been made to investigate the fabrication process and mechanical properties of CNT/Cu composites [10, 18–21]. Up to now, little work has been reported on the thermal properties of CNT/Cu composites. Therefore, the study of their thermal properties has become an important issue that needs to be addressed.

In this study, a dispersion of CNTs in the Cu powders is attempted to use a novel mixing procedure called particle-compositing process. As will be demonstrated in this paper, it is successful to generate composite powders with homogenous distribution of CNTs. The composite powders are consolidated into CNT/Cu composites by using spark plasma sintering (SPS) technique. A main attention is paid for the first time to evaluate the thermal conductivity of CNT/Cu composites.

## Experimental

Materials used in this study were high-purity (99.9%) electrolytic copper powders with 5–10  $\mu\text{m}$  in diameter and multi-walled carbon nanotubes (simply called CNTs hereafter). The average diameter and length of CNTs are 10–30 nm and 5–15  $\mu\text{m}$ , respectively. As-received CNTs were purified in the concentrated nitric acid by performing

the ultrasonic cleaning, then filtered and washed with deionized water and dried at 120°C.

Particles composite system (PCS) was performed for the powders blending experiments. The working principle of PCS [22] is known as particle-compositing process, which is used to convert the different initial particles into composite particles with simultaneous modification of particle properties, including flowability, wettability, dispersability and multifunctional physical properties. A schematic diagram of particles-compositing process is shown in Fig. 1. In such particles-compositing process, high-speed air flow derived from the high-speed rotary blades induces a series of repeating inter-particle actions of impacting, shearing and friction, which allow the particles with large particle sizes (host particles: micron/submicron-level) to be firmly coated with fine particles (guest particles: nanolevel).

The 5 and 10 vol.% CNTs were mixed with Cu powders by PCS at an optimum mixing condition of 5,000 rpm in rotary speed and 40 min in duration. Consolidation was performed by SPS (mod. 1050, Sumitomo Coal Mining Co. Ltd., Japan). The powders were loaded into a graphite die with 30 mm in inner diameter. A sheet of graphitic paper was placed between the punch and the powders as well as between the die and the powders for easy removal. The powders were sintered in a vacuum (less than 5 Pa). The influences of SPS sintering temperature, pressure and holding time were examined. The heating rate was 100°C/min, and a pressure of 40–60 MPa was applied from the start to the end of the sintering. The sintering temperatures were set at 550–650°C with holding times of 5–10 min. A thermocouple, inserted in a little hole at the lateral side of the die, was used to monitor the temperature. The characteristics of the samples were listed in Table 1. For the sake of comparison, a copper specimen, which was sintered using pure copper powders, was used as a reference material.

**Fig. 1** Schematic diagram of particles-compositing process

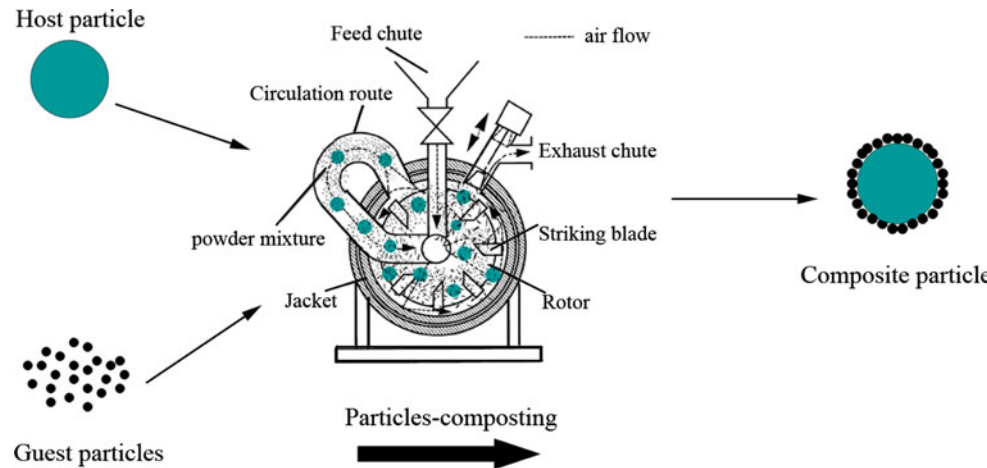


**Table 1** The characteristics of all the samples investigated in this work

Samples	<i>f</i>	<i>T</i>	<i>P</i>	<i>t</i>	RD	TC
A	5%	550	50	5	96.2	283
B		600	50		99	328
C		650	50		99.1	319
D		600	40		96.4	286
E		600	60		99.2	309
F		600	50	10	98.7	319
G	10%	550	50	5	95.3	287
H		600	50		98.8	327
I		650	50		98.6	281
J		600	40		95.3	291
K		600	60		98.9	306
L		600	50	10	98.4	310
Pure copper	–	600	50	5	99	331

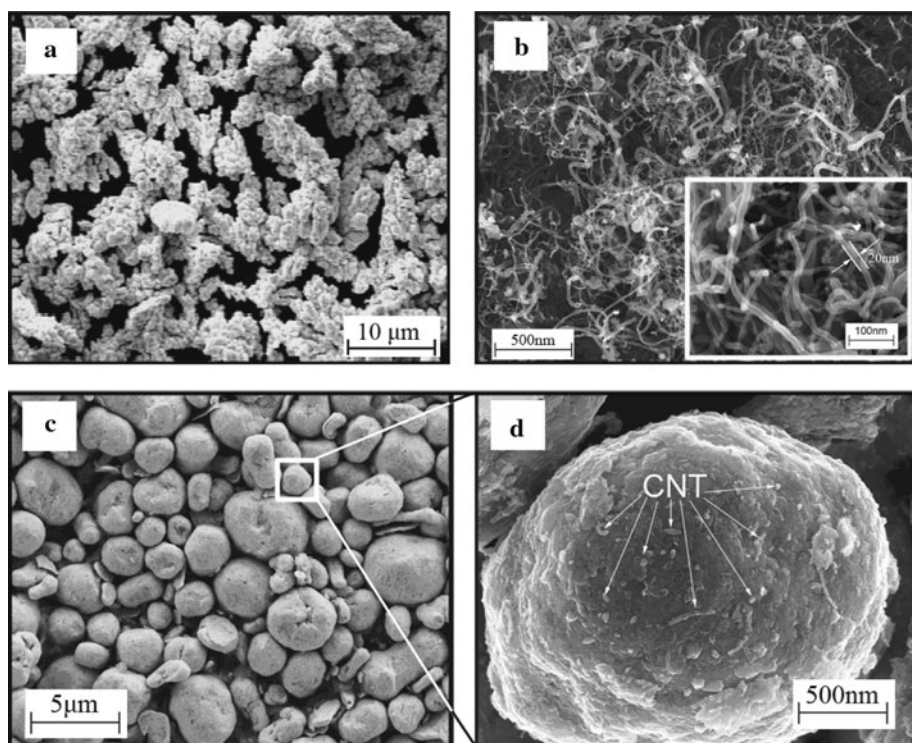
*f* is the CNT volume fraction; *T* is the sintering temperature (°C), *P* is the applied pressure (MPa), *t* is the holding time; RD is the relative density (%), and TC is the thermal conductivity (W/mK)

The microstructure characterization was carried out on a Zeiss Supra55 field emission scanning electron micrograph (FESEM) and an optical microscope. Densities of the consolidated composite specimens were obtained using Archimedes' method with distilled water as the medium. The theoretical densities of pure copper (8.96 g/cm<sup>3</sup>) and CNT (1.75 g/cm<sup>3</sup>, provided by the manufacturer) were used to calculate the relative density of products. The laser

flash method was used to measure thermal diffusivity ( $\alpha$ ) in the JR-3 thermal physical testing instrument. The sample with the size of  $\varnothing 10\text{ mm} \times 3\text{ mm}$  was placed in a chamber, the front of the sample was heated by a laser beam, and the temperature on the rear was recorded by an infrared recorder. The overall measurement confidence interval was assessed as  $\pm 2\%$  of the measured value. The specific heat of the specimens was measured by a differential scanning calorimeter using high-purity single-crystal alumina as a reference material. Thermal conductivity can be then calculated based on the equation  $K = \alpha\rho C_p$ , where  $K$ ,  $\rho$  and  $C_p$  represent thermal conductivity, bulk density and specific heat of the sample, respectively. All measurement results were summarized in Table 1.

## Results and discussion

Figure 2 shows a clear distinction between the morphology of raw powders and composite powders. It can be observed in Fig. 1a, b that the electrolytic Cu powders present a dendritic shape with a rough surface. CNTs are aggregated into ropes or knotted lumps due to strong inter-tube van der Waals attraction, and some of them demonstrate a few local kinks and bends. During the particle-compositing process, the powder mixture is subjected to the high inter-particle collision in a high-speed air flow. The dendritic copper powders are gradually deformed into the spheres, and agglomerated CNT ropes or lumps are disintegrated into the

**Fig. 2** SEM images of **a** as-received copper powders, **b** purified CNTs and **c–d** 10 vol.% CNT/Cu composite powders

individual CNTs that are embedded into the copper spheres. As this process continued, the number of copper spheres and embedded CNTs increases, and the composite powders with uniformly dispersed CNTs are ultimately achieved. As seen in Fig. 2c that the dendritic Cu powders are changed into the spherical ones with a smooth surface after particles-compositing process. The composite powders give homogeneously dispersed CNTs, and most of CNTs are located deeper inside the copper powders rather than on the surface (Fig. 2d). In CNT-reinforced composites, obtaining a uniform dispersion of CNTs in the starting powders is a significant factor affecting the overall properties of the final composites. Many dispersion techniques including mechanical alloying [23], nanoscale dispersion [11], molecular-level mixing [21] and spray drying [24] have been used for dispersing CNTs in the metallic powders. However, nearly all of these techniques aim at the dispersion of CNTs in nano-sized spherical metallic powders. Some of them, such as molecular-level mixing, involve complicated processing steps. In contrast, we can conclude that particles-compositing offers a simple and economical process for uniformly dispersing CNTs within the micron-sized metallic powders that even have an irregular shape.

A considerable number of papers [4, 5, 8, 9] have reported that the incorporation of CNTs into polymers or ceramics can obtain the composites with largely enhanced thermal conductivity. However, it is surprising to find in Table 1 that the thermal conductivities for all the CNT/Cu composites with addition of CNTs are more or less lower than that of CNT-free specimen no matter what the sintering condition is, although the thermal conductivity of MWCNTs (3,000 W/mK) [4] is nearly tenfold higher than that of pure copper sample (331 W/mK). It is worth noting that the powder sintered copper with polycystic structure has much lower thermal conductivity than the monocrystal copper (402 W/mK) due to the existence of grain boundary and defects in polycrystals [25]. The presence of an interfacial thermal resistance between the CNT and the surrounding Cu matrix is believed to be a main reason in causing the measured thermal conductivity to be much less than expected. This interfacial thermal resistance acts as a barrier to the heat flow and thus decreases the overall conductivity. The reported interface resistance values ( $R_K$ ) across the interface of CNT/polymer cover the range of  $2.9\text{--}8.3 \times 10^{-8} \text{ m}^2\text{K/W}$  [26, 27], and these values are of the same order of magnitude as those in CNT/ceramic composites [8]. So far, the value of  $R_K$  accounting for the CNT/metal composites has not been reported to our knowledge. Here, we use an effective medium approach to estimate the  $R_K$  in CNT/Cu composites based on the thermal conductivity measurements.

Nan et al. [28] proposed an analytical model that is applied in order to calculate the thermal conductivity of

CNT-reinforced composites in terms of a general effective medium theory. This model assumes a random orientation of the dispersed CNTs within the matrix and uses an effective medium approach. The effective thermal conductivity of the composite is

$$K_e = K_m \left[ \frac{3 + f(\beta_x + \beta_z)}{3 - f\beta_x} \right] \quad (1a)$$

with

$$\beta_x = \frac{2[d(K_c - K_m) - 2R_K K_c K_m]}{d(K_c - K_m) + 2R_K K_c K_m} \quad (1b)$$

$$\beta_z = \frac{L(K_c - K_m) - 2R_K K_c K_m}{L K_m + 2R_K K_c K_m}$$

Material properties  $K_e$ ,  $K_c$  and  $K_m$  are the thermal conductivities of the composite, the CNT and the matrix, respectively;  $f$  is the CNT volume fraction;  $d$  and  $L$  are the diameter and length of CNT, respectively. In the calculations, the thermal conductivities of copper and CNT are taken to be 331 W/mK (Table 1) and 3,000 W/mK [4], respectively. The average diameter and length of CNTs in composite powders are 20 nm and 10  $\mu\text{m}$  determined by FESEM observations (Fig. 2), respectively. Given these parameters, we then take our best samples (B, H) to fit the theoretical calculations using Eq. (1a) and (1b), and the simulated curves are presented in Fig. 3. The value of  $R_K$  can be determined as  $1.5 \times 10^{-9} \text{ m}^2\text{K/W}$ , which is one order of magnitude lower than that in CNT/polymer or CNT/ceramic composites. For the comparison purpose, we also give the theoretical value of  $K_e$  assuming  $R_K = 0$ . As seen, in the absence of interfacial thermal resistance, the

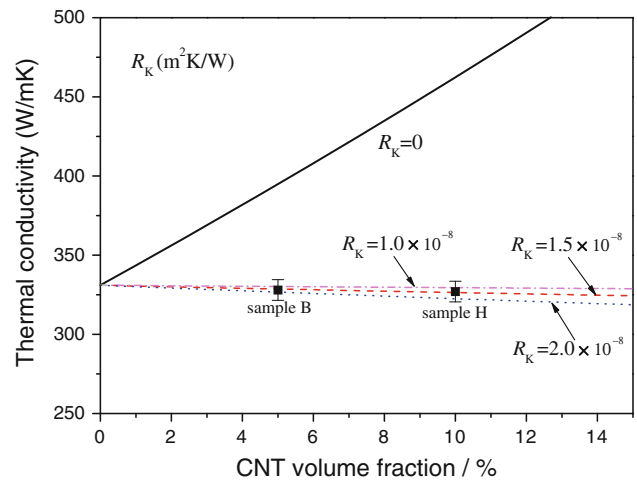


**Fig. 3** Predictions given by the effective medium approach [Eq. (1a) and (1b)] for the thermal conductivity of CNT/Cu composites as a function of CNT volume fraction. The solid line is for the ideal case without the interface thermal resistance. The dotted lines are theoretical values considering the effect of interface thermal resistance. The full squares represent the experimental data

incorporation of CNTs leads to a large enhancement in thermal conductivity. Therefore, it can be deduced that even small interface thermal resistance can greatly limit the heat transport in CNT/Cu composites and result in an exceptionally low value of overall conductivity. Moreover, due to the large impact of interface thermal resistance, the thermal conductivity of the composites is insensitive to the CNT content, where the difference in thermal conductivity of the composites (B, H) with 5 and 10 vol.% CNTs is negligible.

In addition, the degradation in thermal conductivity for other samples is related to the processing parameters during the consolidation by SPS. The effect of sintering temperature on the thermal conductivity and relative density of CNT/Cu composites at a fixed applied pressure of 50 MPa and holding time of 5 min is plotted in Fig. 4. It can be seen that the thermal conductivity increases with the increase in temperature from 550 to 600°C for both composites with 5 and 10 vol.% CNTs, while the noticeable difference is presented when continuously increasing temperature to 650°C, in which the thermal conductivity of 5 vol.% CNT/Cu composite slightly decreases, but the 10 vol.% CNT/Cu composite shows a significant decrease. The low thermal conductivity in 550°C is attributed to the low relative density of the composites (Fig. 4, inset), corresponding to large porosity.

Pores among the Cu grains and the CNTs can compromise the thermal conductivity by enhancement of phonon scattering, therefore to reduce the composite thermal conductivity [29]. The high sintering temperature results in high density and reduces the porosity, therefore, to enhance the thermal conductivity of the composites. The major cause of significant decrease in thermal conductivity of 10

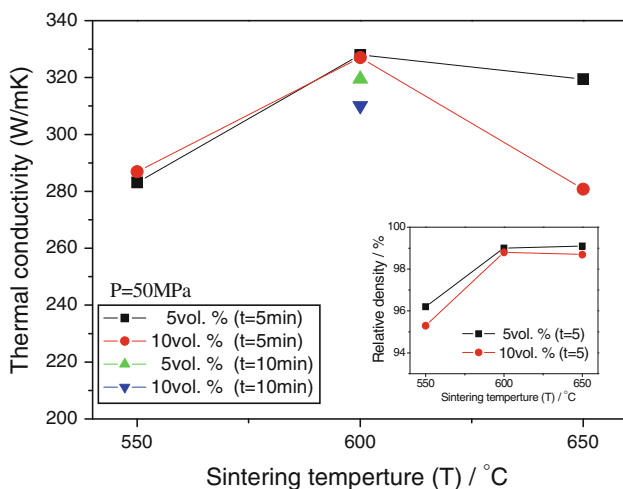


**Fig. 4** The thermal conductivity and relative density (inset) of the composites with 5 and 10 vol.% CNTs as a function of sintering temperature ( $T$ ) at a fixed applied pressure ( $P$ ) of 50 MPa and holding time of 5 min

vol.% CNT/Cu composites at 650°C is not well understood. We propose that it may be related to the segregation of CNTs at the Cu grain boundaries resulted from the matrix grain growth, which can be explained via a schematic diagram of the distribution of CNTs at the Cu grain boundary displayed in Fig. 5 in combination with the microstructural observations. After the composite is fully densified, the growth of matrix grains occurs when continuously increasing temperature (Fig. 5a, b). The grain growth induces the grain rearrangement that leads to the redistribution of CNTs at the grain boundary. As the grain size becomes larger, the volume of grain boundary decreases, and some “redundant” CNTs segregate at the juncture of grain boundary (Fig. 5d). It is well accepted that the phonon–phonon Umklapp scattering makes the major contribution to the thermal conductivity of CNTs [30]. The segregation of CNTs can evoke the intensive tube–tube interactions that can severely suppress Umklapp scattering. The thermal conductivity is thus remarkably decreased. Whereas a low CNT content can effectively avoid the segregation of CNTs during such grain rearrangement process because the most of “redundant” CNTs can fill up the initial CNT-free grain boundary (Fig. 5f). Hence, only a slight decease in thermal conductivity is observed for the composite with 5 vol.% CNTs at 650°C. The increase in holding time also leads to the similar results, as shown in Fig. 4, with the increase in holding time from 5 to 10 min, there is a moderate decease in thermal conductivity. As clear, the effect of holding time is small compared to that of sintering temperature. Although, in most cases, the addition of CNTs can inhibit the matrix grain growth during the sintering process due to the pinning effect of the CNTs [31], the present analyses indicate that this pinning effect of CNTs can be conquered if continuously increasing sintering temperature or prolonging holding time after accomplishing the materials densification. The grain rearrangement can further influence the thermal properties of the composites. However, the further experiments at higher temperature and higher CNT content, which combine the microscope observations, such as TEM or HRTEM studies to carefully examine the presence of CNTs segregation, are necessary for the evaluation of the above explanations.

Figure 6 shows the effect of sintering pressure on the thermal conductivity of CNT/Cu composites at a fixed sintering temperature of 600°C and holding time of 5 min. The thermal conductivity of both composites with 5 and 10 vol.% CNTs increases at first with the CNT content and then decreases when the applied pressure is up to 60 MPa. The increased thermal conductivity is also due mainly to the reduction in porosity (Fig. 6, inset). As mentioned previously, the phonon–phonon Umklapp scattering is the main heat transfer mechanism for CNT, and this Umklapp

**Fig. 5** Distribution of CNTs at the Cu grain boundary at different sintering temperatures and CNT contents. Optical images of 10 vol.% CNT/Cu composites sintered at **a** 600°C and **b** 650°C. Schematics of 10 vol.% CNT/Cu composites at **c** 600°C and **d** 650°C, 5 vol.% CNT/Cu composites at **e** 600°C and **f** 650°C

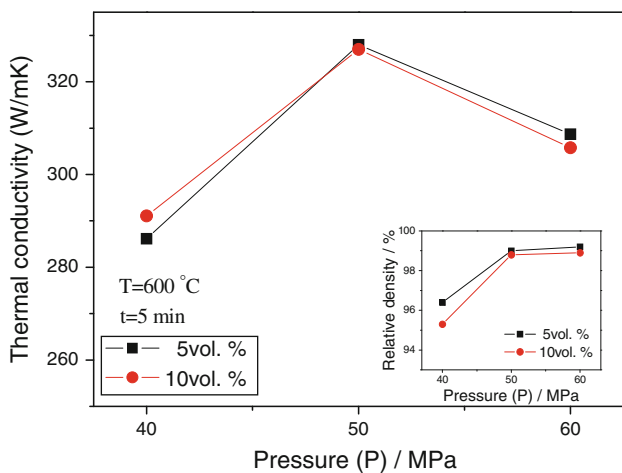
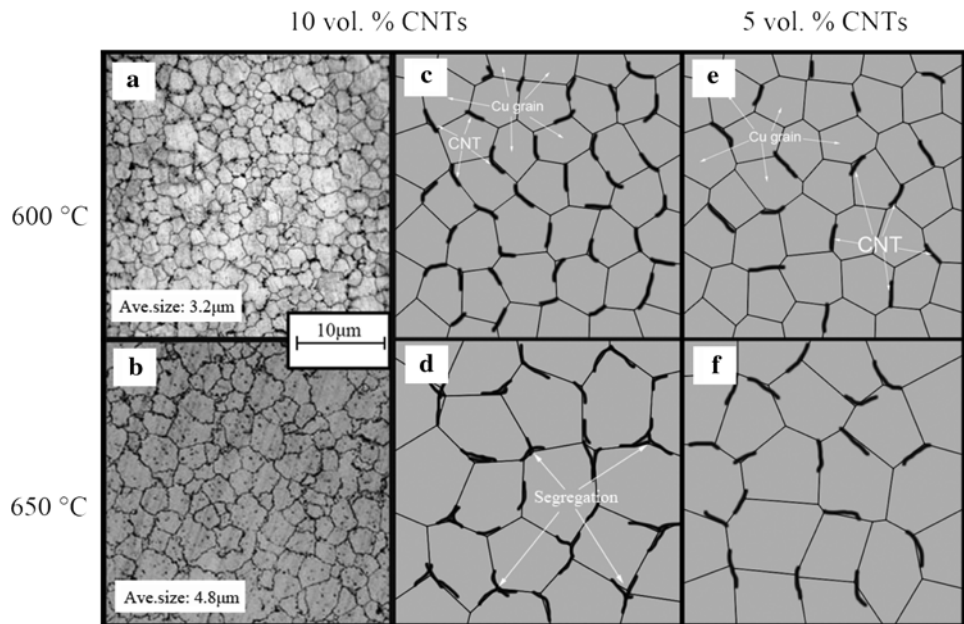


**Fig. 6** The thermal conductivity and relative density (*inset*) of the composites with 5 and 10 vol.% CNTs as a function of applied pressure (*P*) at a fixed sintering temperature of 600°C and holding time of 5 min

scattering would be suppressed in a unidirectional system along longitudinal axis of the nanotube because of the unavailability of states into which to scatter [32]. When the phonon travels along the nanotube, if phonon encounters the kinks or twists, it would be blocked at these sites. The heat loss from this longitudinal heat transport thus reduces the overall conductivity. It is generally known that most of CNTs are naturally kinked or twisted, the pressure applied during SPS processing can cause the CNTs to be further kinked or twisted [33], and these kinks or twists would be increased with increasing pressure. Consequently, the large number of kinks or twists largely offsets the benefit of the high thermal conductivity of CNT, giving rise to a great

degradation in thermal conductivity. According to our measurements, it can be inferred that the moderate pressure does not lead to a marked increase in kinks or twists, while the pressure like 60 MPa is high enough to induce the occurrence of massive kinks or twists that could considerably decrease the thermal conductivity of the composites.

The CNT/Cu composites have attracted the interest of many researchers for their excellent mechanical properties. On the other hand, it is of interest to point out that CNT/Cu composites may find thermal management applications based on their superior thermal properties. In these applications, there are two main requirements: a high thermal conductivity and a low coefficient of thermal expansion (CTE) similar to that of semiconductor materials. The present study suggests that the incorporation of CNTs can still maintain the high thermal conductivity of the copper via the prescribed fabrication procedures. Actual measurements of CNT/Cu composites show a maximum thermal conductivity of 328 W/mK, which is much better than that of commercialized W-Cu(Mo) or SiC/Al(Cu) materials [34]. With respect to the CTE, although the investigations into the CTE of CNT/Cu composites have not been reported, a recent research on the CTE of CNT/Al composites demonstrated that the addition of 15 vol.% CNTs to Al reduced the CTE of Al matrix by as much as 65% [35]. It is noted that the CTE of copper is 30% lower than that of aluminum; one can expect that the addition of CNTs in Cu matrix would lead to a further reduced CTE. Therefore, the high thermal conductivity and low CTE will push CNT/Cu composites up in the list of candidates being considered for thermal management applications. However, the high price of CNT and fabrication limitations may still be an issue for their applications.

## Conclusions

The CNT/Cu composite powders with homogeneously dispersed CNTs were fabricated by means of a novel particles-compositing process, which were fully densified by subsequent SPS technique. The thermal conductivity of the composites was not enhanced by the incorporation of CNTs. Besides the effect of sintering condition, the existence of interface thermal resistance between the CNT and the Cu matrix was considered to be the main reason for this unexpected low thermal conductivity. The thermal conductivity predictions obtained from the effective medium approach revealed that only small interface thermal conductance can cause a significant degradation in thermal conductivity for CNT/Cu composites. The composites sintered at 600°C for 5 min under 50 MPa showed the maximum thermal conductivity. At lower sintering temperatures (below 600°C) or pressure (below 50 MPa), the increases in both temperature and pressure enhanced the composite conductivity attributed to porosity removal. At higher temperatures above 600°C, the composite conductivity decreased with increasing sintering temperature and holding time, and this degradation was enhanced with the increase in CNT content. It was suggested that the presence of CNTs segregation formed in the matrix grain rearrangement process may be a main disadvantage for resulting in the reduction in thermal conductivity at higher temperature. The high pressure (60 MPa) reduced the composite conductivity due to the inducement of massive kinks or twists in CNTs. The present study implies that the CNT/Cu composites may have potential applications in the field of thermal management.

**Acknowledgments** This study was financially supported by National Natural Science Fund of China (No. 50971020) and National 863 Plan Project of China (No. 2008AA03Z505).

**Open Access** This article is distributed under the terms of the Creative Commons Attribution Noncommercial License which permits any noncommercial use, distribution, and reproduction in any medium, provided the original author(s) and source are credited.

## References

1. S. Iijima, Nature **354**, 56 (1991)
2. E.T. Thostenson, Z.F. Ren, T.W. Chou, Compos. Sci. Technol. **61**, 1899 (2001)
3. R.H. Baughman, A.A. Zakhidov, W.A. de Heer, Science **297**, 787 (2000)
4. M.J. Biercuk, M.C. Llaguno, M. Radosavljevic, J.K. Hyun, A.T. Johnson, Appl. Phys. Lett. **80**, 2767 (2002)
5. C.H. Liu, H. Huang, Y. Wu, S.S. Fan, Appl. Phys. Lett. **84**, 4248 (2004)
6. S.L. Ruan, P. Gao, X.G. Yang, T.X. Yu, Polymer **44**, 5643 (2003)
7. G.D. Zhan, J.D. Kuntz, J. Wan, A.K. Mukherjee, Nat. Mater. **2**, 38 (2003)
8. L. Kumari, T. Zhang, G.H. Du, W.Z. Li, Q.W. Wang, A. Datye, K.H. Wu, Compos. Sci. Technol. **68**, 2178 (2008)
9. R. Sivakumar, S.Q. Guo, T. Nishimura, Y. Kagawa, Scripta Mater. **56**, 265 (2007)
10. S.I. Cha, K.T. Kim, S.N. Arshad, C.B. Mo, S.H. Hong, Adv. Mater. **17**, 1377 (2005)
11. T. Noguchi, A. Magario, S. Fukazawa, S. Shimizu, J. Beppu, M. Seki, Mater. Trans. **45**, 602 (2004)
12. T. Laha, A. Agarwal, T. McKechnie, S. Seal, Mater. Sci. Eng A **381**, 249 (2004)
13. E. Carreno-Morelli, J. Yang, E. Couteau, K. Hernadi, J.W. Seo, C. Bonjour, L. Forró, R. Schaller, Phys. Status Solidi A **201**, 53 (2004)
14. B.K. Jang, Mater. Lett. **63**, 2545 (2009)
15. S. Wang, R. Liang, B. Wang, C. Zhang, Carbon **47**, 53 (2009)
16. Y. Yosida, J. Appl. Phys. **8**, 3338 (2000)
17. S. Berber, Y.K. Kwon, D. Toma'nek, Phys. Rev. Lett. **84**, 4613 (2000)
18. S.R. Dong, J.P. Tu, X.B. Zhang, Mater. Sci. Eng A **313**, 83 (2001)
19. K.T. Kim, S.I. Cha, S.H. Hong, Mater. Sci. Eng A **449–451**, 46 (2007)
20. P. Quang, Y.G. Jeong, S.C. Yoon, S.H. Hong, H.S. Kim, J. Mater. Process. Tech. **187–188**, 318 (2007)
21. C. Kima, B. Lima, U. Shima, S. Ohb, B. Sunga, J. Choia, J. Kia, S. Baika, Synthetic Met **159**, 424 (2009)
22. G.S. Gai, Y.F. Yang, L. Jin, X. Zou, Y.X. Wu, Powder Technol. **183**, 115 (2008)
23. N. Pierard, A. Fonseca, Z. Kenya, I. Willems, G. Van Tendeloo, J.B. Nagy, Chem. Phys. Lett. **335**, 1 (2001)
24. S.R. Bakshi, V. Singh, S. Seal, A. Agarwal, Surf. Coat. Tech. **203**, 1544 (2009)
25. C.W. Nan, R. Birringer, Phys. Rev. B **57**, 8264 (1998)
26. S. Huxtable, D.G. Cahill, S. Shenogin, L. Xue, R. Ozisik, P. Barone, M. Usrey, M.S. Strano, G. Siddons, M. Shim, P. Kebinski, Nat. Mater. **2**, 731 (2003)
27. M. Foygel, R.D. Morris, D. Anez, S. French, V.L. Sobolev, Phys. Rev B **71**, 104201 (2005)
28. C.W. Nan, G. Liu, Y.H. Lin, M. Li, Appl. Phys. Lett. **85**, 3549 (2004)
29. B.K. Jang, J. Alloys. Compd. **480**, 806 (2009)
30. D.T. Morelli, J. Heremans, M. Sakamoto, C. Uher, Phys. Rev. Lett. **57**, 869 (1986)
31. H. Kwon, M. Estili, K. Takagi, T. Miyazaki, A. Kawasaki, Carbon **47**, 570 (2009)
32. M.S. Dresselhaus, G. Dresselhaus, P. Avouris, *Carbon nanotubes: synthesis, structure, properties, and applications* (Springer, Berlin, 2001)
33. H.L. Zhang, J.F. Li, K.F. Yao, L.D. Chen, J. Appl. Phys. **97**, 114310 (2005)
34. M. Robins, Electron. Packag. Prod. **40**, 50 (2000)
35. Y.B. Tang, H.T. Cong, R. Zhong, H.M. Cheng, Carbon **42**, 3251 (2004)